ORIGINAL ARTICLE

Preparation, Characterization and *in Vitro* Drug Release Evaluation of Chitosan Nanoparticles for Atovaquone

Ahmad Basim Alasas, Noratiqah Mohtar and *Amirah Mohd Gazzali

School of Pharmaceutical Science, Universiti Sains Malaysia, 11800 USM Penang, Malaysia

ABSTRACT

Introduction: The classification of atovaquone (ATQ) as a BCS Class II drug illustrates its solubility challenges in the GIT that will affect its oral absorption and bioavailability. Among the polymers available for nanoparticles production, chitosan has demonstrated favorable properties, including biocompatibility and low toxicity. The objective of this study is to prepare and characterize chitosan nanoparticles as a carrier for ATQ with a specific aim for solubility enhancement. **Methods:** ATQ-loaded chitosan nanoparticles were prepared using the ionic gelation method. The formulations were characterized for particle size, polydispersity index (PDI), surface charge, encapsulation efficiency, FTIR spectroscopy, and in vitro drug release study in simulated gastric fluid (SGF; pH 1.2) and simulated intestinal fluid (SIF; pH 6.8). The stability of the nanoparticles was evaluated at 4°C, 25°C, and 40°C/75%RH for three months. **Results:** The physical properties of chitosan nanoparticles can be controlled by manipulating the components used in the formulation. The final formulation features: a particle size of 235.9 nm (± 4.9), PDI of 0.26 (± 0.02), zeta potential of +29.2 mV (± 1.1), and an encapsulation efficiency of 95.0% (± 1.0). In vitro drug release study showed a 7-fold and 4-fold increase in the solubility of ATQ in SGF and SIF respectively, as compared to the free drug. The aqueous nanoparticle formulations were stable for three months at 4°C and 25°C storage conditions. **Conclusion:** This study highlights the ability of chitosan nanoparticles to enhance the solubility of ATQ and potentially increase the bioavailability of ATQ *in vivo*.

Keywords: Chitosan; Atovaquone; Nanoparticles; Experimental design; Tripolyphosphate

Corresponding Author:
Amirah Mohd Gazzali, Ph.D
Email: amirahmg@usm.my
Tel: +604-653 3888

INTRODUCTION

Atovaquone is an antiprotozoal drug with a broad-spectrum activity. It is active against *Plasmodium species*, *Toxoplasma gondi*, *Leishmania species*, *Pneumocystis carinii*, and Babesia species (1). ATQ is an FDA-approved drug for preventing malaria and treating pneumocystis pneumonia and toxoplasmosis in HIV patients (2), besides is active in the hepatic stages of *Plasmodium falciparum* (3). The structure of ATQ is an analog of ubiquinone, also widely known as Coenzyme Q, which plays an important role in the electron transport at cytochrome bc1 complex in the parasite mitochondria (4). ATQ acts by selectively inhibiting the electron transport in the mitochondria respiratory chain of the malarial parasites, at the cytochrome bc1 complex. In addition, ATQ also destroys the electro-potential activity across the inner mitochondrial membrane that would subsequently lead to cell death or apoptosis (5, 6).

ATQ (pKa value = 8.23) is classified as a Class II drug - low solubility and high permeability- according to the Biopharmaceutics Classification System (BCS) (7). This classification represents the problem surrounding the solubilization of ATQ in the GIT that would directly affect its absorption into the blood circulation following oral administration and eventually will affect its bioavailability, requiring higher doses for effective antimalarial action, possibly contributing to drug resistance due to suboptimal drug concentrations resulting from insufficient absorption (8, 9).

Chitosan (CS) is a cationic polysaccharide that is derived from chitin through an alkaline N-deacetylation process. Chitin, in turn, can be obtained from various sources, including fungal mycelia as well as the shells of crabs and shrimps (10, 11). Chitosan's favorable properties, including low toxicity, excellent biocompatibility, biodegradability, and a positive charge, make it an attractive material for drug delivery, with remarkable bioadhesive characteristics and permeation enhancement effects (12). There are several preparation methods for chitosan nanoparticles reported in the literature. This includes emulsification and cross-linking (13), ionic gelation (14), polyelectrolyte complexation (15), desolvation (16), and reverse micellization (17). Among these methods, the ionic gelation method (first described by Calvo et al. (1997)) is particularly attractive for chitosan nanoparticle preparation due to its mild and

simple process, utilizing physical cross-linking instead of potentially toxic chemical cross-linking reagents, making it a safer alternative (18). The method is based on electrostatic interaction between chitosan's amine group (positive charge) and polyanions (negative charge) from the crosslinker, in which the addition of tripolyphosphate (TPP) into chitosan solution has been shown to lead to spontaneous nanoparticles formation under stirring condition. (19, 20). TPP is widely used as the polyanion in ionic gelatin method because of its low toxicity and relatively lower cost as compared to other polyanions, besides being easy to handle and having simple storage requirements (21).

This article describes the preparation and optimization of the formulation of chitosan nanoparticles by determining the effect of changing the concentration of components (i.e., chitosan, acetic acid, and TPP) on the physical properties of the chitosan nanoparticles. ATQ has a challenging physicochemical characteristic as a BCS Class II drug. Thus, the ability of chitosan nanoparticles as a drug carrier will be evaluated in improving the solubility of ATQ, besides its potential in preserving the stability of the loaded ATQ during storage.

MATERIALS AND METHODS

Chitosan (low molecular weight or LMW, approximately 150,000 Da) was obtained from Fluke® (Malaysia). Acetic acid glacial was obtained from Systerm® (Malaysia), whereas TPP sodium was purchased from R&M® (Malaysia). Sodium hydroxide (NaOH) was obtained from AnalaR® (United Kingdom), and ATQ was obtained from Hallochem® (China). Tween®80 was obtained from EURO® (Malaysia), whereas poloxamer 188 was purchased from Molekula® (United Kingdom).

Pre -formulation study – The preparation of chitosan nanoparticles by design of experiment approach

The design of experiment approach was used to optimize the parameters used in the production of chitosan nanoparticles. Design-Expert® software version 12 (Stat-Ease Inc., United States) was used to generate 17 experiments using "Mixture design" with the following concentrations ranges: acetic acid (Component A: 0.10–0.30 % w/v), chitosan (Component B: 0.05–0.20 % w/v) and TPP (Component C: 0.05–0.08 % w/v). The set responses were particle size (nm), zeta potential (mV), and PDI.

Chitosan nanoparticles were prepared according to the ionic gelation method (19) with some modifications. The specified amount of chitosan (g) was dissolved in an acetic acid solution with the aid of water bath sonication until a clear solution was obtained. The pH of the solution was adjusted to 4.6 with 0.1M sodium hydroxide (NaOH). Separately, the TPP solution was prepared by dissolving TPP in distilled water under stirring at 600 rpm until complete dissolution. To produce chitosan nanoparticles, TPP solution was added dropwise into the chitosan solution under stirring (600rpm) at room temperature at a 3:1 mass ratio (chitosan: TPP). The mixture was then stirred for an additional one hour. The mixture was neutralization using one M NaOH, whilst the unformed materials were separated using centrifugation at 4000 rpm for ten mins (21-24).

Characterization

The average particle size and PDI of chitosan nanoparticle was measured using Litesizer 100 (Anton Paar®, Austria) which uses the concept of dynamic light scattering (DLS) in the measurement. The analysis was conducted at 25 °C. Standard cuvette cells with 10 mm x 10 mm x 45 mm inner dimensions were used. Surface charge (Zeta potential) was measured using Nano-series Zetasizer (Malvern Instruments, United Kingdom) at 25°C. DTS1070 cell was used in the measurement.

Preparation of ATQ-loaded Chitosan Nanoparticles

Based on the results obtained from the pre-formulation study, three chitosan nanoparticle formulations with the best characteristics in terms of particle size, PDI, and zeta potential were chosen for the ATQ-loading study. Three ATQ: CS ratios were prepared for each formula (1:20, 1:50, 1:100) and each loading was done in triplicate (n=3).

The drug loading was done as follows: The specified amount of chitosan (g) was dissolved in an acetic acid solution and separately ATQ was dissolved in 0.1 M NaOH and 0.01 mg/ml Tween® 80. The two solutions were mixed under continuous stirring and TPP solution was added dropwise into the solution and stirred (600 rpm) for one hour at room temperature. The mixture was neutralized using one M NaOH and the unformed materials were then separated using centrifugation at 4000 rpm for ten mins.

Characterization of ATQ-loaded chitosan nanoparticles

The physical characterizations of the ATQ-loaded chitosan nanoparticles include the determination of particle size (nm), PDI, surface charge, encapsulation efficiency (%), Fourier transform infrared (FT-IR) spectroscopy, in vitro drug release, and stability study.

Determination of encapsulation efficiency

The encapsulation of ATQ in the nanoparticles was determined as follows: one mL of ATQ-loaded chitosan nanoparticles was mixed with four mL of methanol and the mixture was sonicated for five mins then filtered using 0.2 µm PTFE syringe filter and the filtrate was injected into the HPLC system. The amount of ATQ was determined using a validated HPLC method (25).

Encapsulation efficiency (% EE) was then calculated using Equation 1:

$$\% \text{ EE} = \frac{\text{Weight of encapsulated atovaquone (g)}}{\text{Initial weight of atovaquone (g)}} \text{ X } 100\%$$

Equation 1: Formula for encapsulation efficiency (%) calculation.

Fourier transform infrared (FT-IR) spectroscopy

The FT-IR spectrum of chitosan, blank chitosan nanoparticles, ATQ, and ATQ-loaded chitosan nanoparticles was evaluated using the Nicolet Nexus 470 FTIR spectrometer (Thermo, USA). FT-IR was used to detect the functional groups and identify the chemical bonds between molecules, which will provide valuable information about material composition and interaction. The sample was mixed and ground with KBr (at a weight ratio of 1:100), before being pressed into a thin disc (26). The recording was set at 4 cm^{-1} resolution, 32 scans with a transmission mode between 400 cm^{-1} and 6000 cm^{-1}. The data obtained were analyzed using Spectragryph® (Germany) software version 1.2.14.

***In vitro* drug release study**

One formulation with optimal characteristics was chosen to be evaluated in the in vitro drug release study, in comparison to the unformulated ATQ (free drug). The release study was conducted using a dialysis membrane diffusion method (with a molecular cut-off 12-14 kD,) in 650 mL simulated gastric fluid (SGF) (without enzymes) pH 1.2 and simulated intestinal fluid (SIF) (without enzymes) pH 6.8. Both media were prepared according to the United States Pharmacopeia (USP) as previously described by other researchers (25, 27-29). To improve the wetting of the ATQ, 1% w/w poloxamer 188 was added to the release medium, and the study was conducted at 37 ± 2°C under a stirring of 100 rpm (25).

At predetermined time intervals, one mL aliquot was withdrawn and filtered using a 0.2 µm PTFE syringe filter, and the filtrate was injected into the HPLC system to quantify the amount of ATQ released from the nanoparticles. The withdrawn aliquots were immediately replaced with an equal volume of fresh dissolution media. All evaluations were done in triplicate using HPLC analysis (n=3).

Stability study

The final formulation was placed in universal bottles, protected from light, and stored at 2-4°C (refrigerator), 25°C (room temperature), and 40°C/75%RH (humidity chamber) for three months. Samples were analyzed at 0, 15, 30, 45, 60, and 90 days to determine any changes in the particle size, PDI, zeta potential and total drug content. The total drug content was evaluated using a validated HPLC method (25). The most suitable storage condition for the nanoparticles was determined at the end of the study.

Statistical analysis

T-test and Analysis of Variance (ANOVA) were performed by using SPSS software to compare between results. P-values of less than 0.05 are accepted as statistically significant.

RESULTS

Design-Expert® 12

The results obtained are outlined in Table I. There were 17 experimental runs suggested by the Design-Expert® software to evaluate the influence of the three components (concentrations of acetic acid, chitosan, and TPP) on the characteristics of chitosan nanoparticles produced. Of the 17 experiments, six could not be completed due to the insolubility of chitosan at the concentration of acetic acid used. Most of the formulas suggested have successfully produced nanoparticles of less than 300 nm, except Run #8 which produced the largest particles (465.4 nm), whilst the smallest particles were given by Run #9 (148.4 nm). All runs showed sufficiently good PDI, indicating a good uniformity of the particles. In terms of surface charge, seven out of the 11 successful runs showed a zeta potential higher than +30 mV, whilst four runs showed otherwise. Run #8 gave the lowest zeta potential value, which was recorded as +17.9 mV.

Based on the responses recorded, the Design Expert® software predicted the relative impact of each component on the characteristics of the nanoparticles produced. Coded equations were generated to link the components to their impact (Equation 2, 3, and 4). In general, a positive value in the equations will lead to an increase in the response, and *vice versa*:

Particle size = (-24.4422) * A +(+576.184) * B +(+20959.4) * C +(+1884.57) * AB +(+28393.8) * AC +(+ 39168.5) * BC +(-39680.8) * ABC

Equation 2: Equation summarizes the effect of each tested parameter on the size of chitosan nanoparticles (A = Acetic acid, B = Chitosan, C=TPP)

Zeta potential = (+ 24.932) * A +(+ 43.428) * B +(-193.183) * C +(+ 19.985) * AB +(+ 189.134) * AC +(-340.598) * BC +(+ 1300.539) * ABC

Equation 3: Equation summarizes the effect of each tested parameter on the zeta potential of chitosan nanoparticles (A = Acetic acid, B = Chitosan, C=TPP)

PDI = (- 0.23048) * A +(+ 0.220487) * B +(+2.31547) * C +(+ 0.137943) *AB +(+ 3.36468) * AC +(+3.90156) * BC +(-3.13504) * ABC

Equation 4: Equation summarizes the effect of each tested parameter on the PDI of chitosan nanoparticles (A = Acetic acid, B = Chitosan, C=TPP)

Table I : Responses (particle size (nm), PDI and zeta potential (mV)) recorded for each formula generated by Design-Expert® 12.

	Component 1	Component 2	Component 3	Response 1	Response 2	Response 3
Run #	A: Acetic acid %	B: Chitosan %	C: TPP %	Particle size (nm)	PDI	Zeta potential (mV)
1	0.22	0.13	0.05	200.0 ± 8.6	0.26± 0.01	+ 37.8 ± 1.3
2	0.21	0.12	0.06	266.3 ± 22.4	±0.27 0.01	+40.0 ± 1.2
3	0.21	0.12	0.06	252.9 ± 33.7	0.27 ± 0.02	+36.2 ± 1.4
4	0.21	0.12	0.06	233.8 ± 23.6	0.26 ± 0.02	+37.9 ± 1.9
5	0.13	0.20	0.07		*	
6	0.20	0.15	0.05		*	
7	0.18	0.15	0.08		*	
8	0.28	0.05	0.07	465.4 ± 43.0	0.28 ±0.03	+17.9 ± 1.2
9	0.24	0.09	0.08	148.4 ±13.5	0.25 ±0.01	+33.2 ± 3.6
10	0.13	0.20	0.07		*	
11	0.20	0.12	0.08	183.3±14.2	0.24 ±0.01	+30.6 ± 1.3
12	0.15	0.20	0.05		*	
13	0.29	0.05	0.05	157.9 ± 23.9	0.26 ± 0.02	+24.2 ± 2.7
14	0.29	0.05	0.05	152.5 ± 22.0	0.24 ±0.01	+26.1 ± 2.5
15	0.27	0.08	0.05	162.3 ±18.5	0.25 ± 0.01	+31.6 ± 3
16	0.21	0.12	0.06	249.9 ± 24.5	0.26 ±0.02	+37.1 ±2.2
17	0.17	0.18	0.05		*	

*The combination of components proposed by Design-Expert® 12 failed to solubilize chitosan for nanoparticles production. Thus, nanoparticle-related data could not be recorded for this run #.
Note: All experiments were done in triplicate (n = 3)

Table II : Three formulations with the best physical properties from Design– Expert® 12 trials

Run	Acetic acid (% v/v)	Chitosan (%m/v)	TPP (%m/v)	Particle size (nm)	PDI	Zeta potential (mV)
9	0.24	0.09	0.08	148.4 ± 13.5	0.25 ± 0.01	+ 33.2 ± 3.6
14	0.29	0.05	0.05	152.5 ± 22.0	0.24 ± 0.01	+ 26.1 ± 2.5
15	0.27	0.08	0.05	162.3 ± 18.5	0.25 ± 0.01	+ 31.6 ± 3.0

Table III Characteristics of ATQ-loaded chitosan nanoparticles

Run	ATQ: CS ratio	Particle size (nm)	PDI	Zeta potential (mV)	EE (%)
9	1:20	577.5 ± 64.0	0.37 ± 0.02	+ 7.8 ± 0.12	30.9 ± 4.5
	1:50	477.1 ± 46.0	0.33 ± 0.02	+ 17.2 ± 0.9	58.6 ± 14.3
	1:100	286.6 ± 5.5	0.28 ± 0.01	+ 19.3 ± 1.4	93.4 ± 3.0
14	1:20	>1000	0.37 ± 0.03	+ 10.1 ± 1.7	36.9 ± 9.5
	1:50	460.4 ± 81.2	0.33 ± 0.02	+ 15.3 ± 2.3	58.5 ± 13.0
	1:100	288.0 ± 44.7	0.27 ± 0.01	+ 21.5 ± 1.3	83.5 ± 2.7
15	1:20	>1000	0.41 ± 0.06	+ 13.8 ± 1.7	20.8 ± 7.9
	1:50	466.3 ± 127	0.33 ± 0.04	+ 22.2 ± 1.9	34.4 ± 3.4
	1:100	235.9 ± 4.9	0.26 ± 0.02	+ 29.2 ± 1.1	95.0 ± 1.0

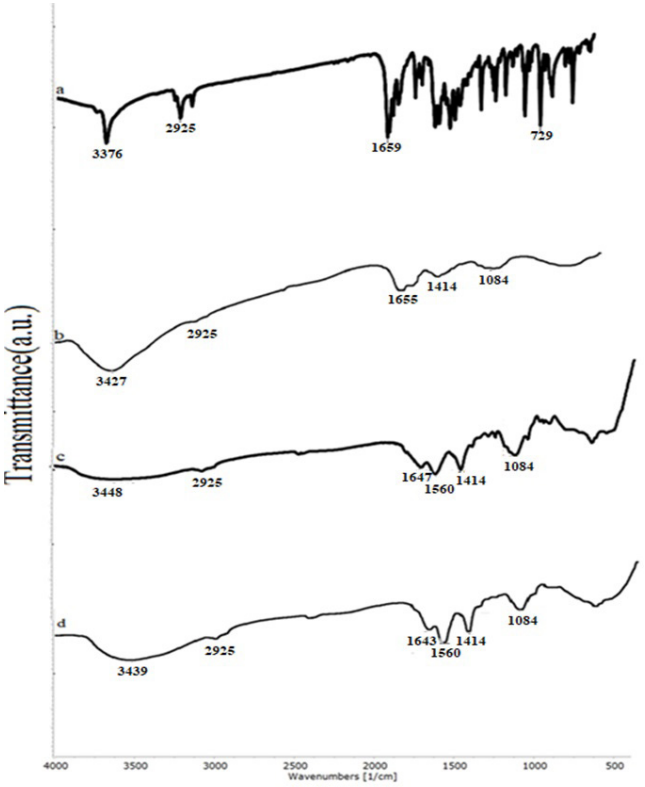

Figure 1 : FTIR spectra (resolution 4 cm^{-1}) of (a) ATQ powder, (b) chitosan flakes, (c) chitosan nanoparticles (blanks), and (d) ATQ-loaded chitosan nanoparticles (Run #15, 1:100 ratio).

A positive value in the equations will lead to an increased response, and vice versa. This means that an increase in the concentration of chitosan (positive value, Component A) will cause an increment in the surface charge, while an increase in the concentration of TPP (negative value, Component C) will lead to a reduction in the surface charge (Equation 3).

Preparation and characterization of ATQ-loaded chitosan nanoparticle

Based on the findings from the previous section, three formulations were chosen to be evaluated in the ATQ-loading experiment (Table II). Three ATQ:CS concentration ratios were prepared for each formula (1:20, 1:50, 1:100) and each experiment was done in triplicate (n=3). The quantification of ATQ loaded in the chitosan nanoparticles was analyzed by HPLC to determine EE (%). The result obtained is presented in Table III.

Fourier-Transform Infra-Red (FTIR) spectroscopy

Figure 1 illustrates the FTIR spectra of chitosan flakes, chitosan nanoparticles (blank), ATQ, and ATQ-loaded chitosan nanoparticles (Run #15, 1:100 ratio).

ATQ displayed characteristic peaks at specific wavenumbers: 3376 cm-1 (hydroxyl group O-H stretching), 2925 cm-1 (aromatic ring C-H stretching), 1659 cm-1 (aromatic ketone C=O stretching), and 729 cm-1 (phenyl ring C-Cl stretching) (30) (31). The

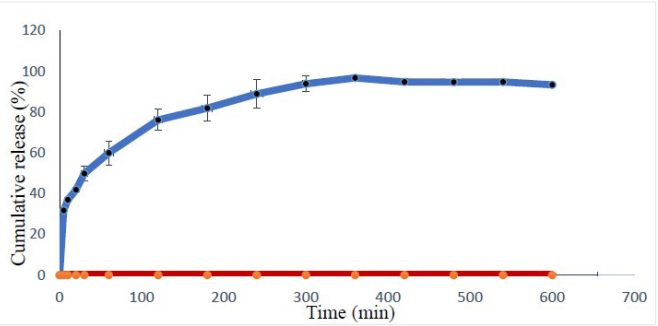

Figure 2 : *In vitro* release of ATQ (red line) from ATQ-loaded chitosan nanoparticles (blue line) in SGF (pH 1.2).

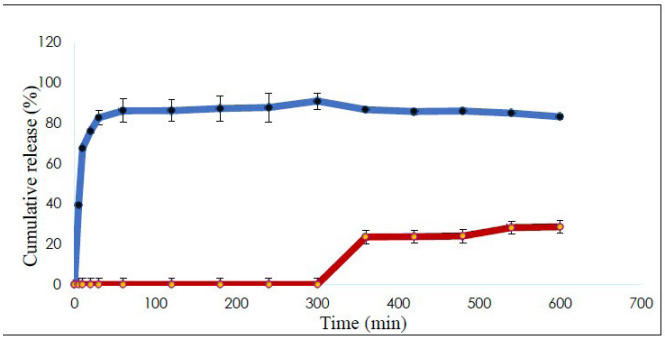

Figure 3 : *In vitro* release of ATQ (red line) from ATQ-loaded chitosan nanoparticles (blue line) in SIF (pH 6.8).

spectrum of the chitosan flakes (b) reflects the abundance of -OH and -NH groups in the substructure as the broad peak at 3427 cm^{-1}, which corresponded to the stretching vibration of O-H and N-H. Four other peaks that are present include the peaks at 2925 cm^{-1} (C-H stretching), 1655 cm-1 (C=O bending vibration), 1414 cm^{-1} (O-H deformation bending vibration), and 1084 cm^{-1} (C–O stretching vibration) (23). In the spectrum of chitosan nanoparticles (blank) (c), the O-H/N-H vibration peak was shifted from 3427 cm^{-1} to 3448 cm^{-1}. The amide was shifted to 1647 cm^{-1} from 1655 cm^{-1} and a new peak appeared at 1560 cm^{-1}. Following the loading of ATQ, some peaks were shifted such as 1647 cm^{-1} was shifted to 1643 cm^{-1} and the peak at 3448 cm^{-1} was shifted to 3439 cm^{-1}.

***In vitro* release study**

The in vitro release behavior of ATQ-loaded chitosan nanoparticles (Run #15 with 1:100 ratio (ATQ: CS)) in both buffered media showed an initial burst release, (Figure 2 & Figure 3). In general, the release of ATQ in SGF is much slower. The burst release observed reached 50% at 30 minutes, followed by a more sustained release until six hours when the release reached a plateau. In comparison to the free drug, ATQ-loaded nanoparticles showed 96.7% (±1.1%) drug release in six hours (SGF) and 90.8% (±6.9%) in five hours (SIF). On the other hand, non-formulated ATQ (free drug) achieved 29.3% (±4.1%) solubility in SGF and 49.1 % (±4.5%) in SIF in 24 hours.

Stability study

The stability of the ATQ-loaded nanoparticles was evaluated at three different storage conditions (4°C, 25°C, and 40°C/75% RH) for three months, in which the particles' physicochemical characteristics including particle size, PDI, zeta potential and total drug content was evaluated at predetermined time points. The particle size remained consistent, measuring less than 300 nm at both 4°C and 25°C with no significant changes in the PDI. Zeta potential was also maintained at over +20 mV under both storage conditions. However, when stored at 40°C with 75% RH, significant changes were observed. The particle size decreased from an initial measurement of 242.3 nm (±2.0 nm) to 103.0 nm (±3.7 nm), accompanied by a notable shift in the PDI. Moreover, the zeta potential dropped from +30.4 mV (±1.0 mV) to +12.5 mV (±1.2 mV).

The total drug content was evaluated at each time point and the finding is illustrated in Figure 4. The total drug content was maintained at 98.5% (±0.5%) and 94.4% (±0.9%) following storage for three months at 4°C and 25°C, respectively. However, a significant reduction ($p < 0.05$) in the drug content was seen in the first month of storage at 40°C/75%RH followed by a gradual decrease in the next two months. At the end of the three months, the remaining amount of ATQ recorded was 25.4% (±2.1%).

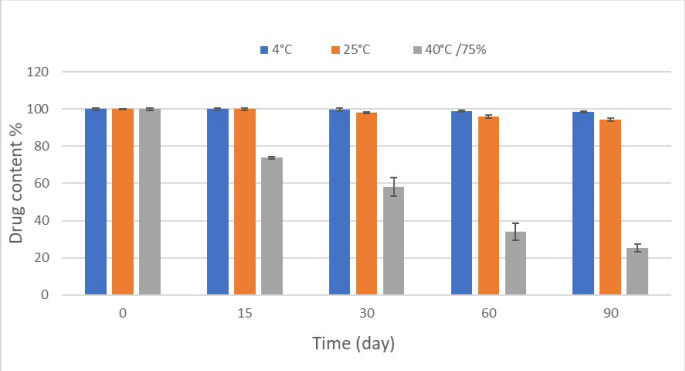

Figure 4 : The changes in total drug content (%) of ATQ-loaded chitosan nanoparticles following storage at three different conditions (4°C, 25°C, and 40°C/75%RH) for three months.

DISCUSSION

Mixture designs are commonly used when the product under study is made of several components or ingredients in which the response is a function of the proportions of each component in the mixture (32). In several cases, the adjustment of proportions is essential to obtain the desired output. Mixture design is an efficient method to establish the proportions of ingredients, or variables in a blend. Although there is no multipurpose technique that can be used in every situation, mixture designs have been effectively used in scientific research and development (33).

As observed in Table I and indicated by Equations 2 and 4, the particle size and PDI increase with an increase in chitosan concentration. This can be attributed to the increased intermolecular interaction between chitosan molecules, leading to the accumulation of chitosan molecules within the formulation. Specifically, the presence of protonated amino groups in chitosan results in electrostatic repulsion between chitosan molecules. However, there are also interchain hydrogen bonding interactions between chitosan molecules. With an increase in chitosan concentration, the strength of hydrogen bonding interactions becomes stronger than the electrostatic repulsion, resulting in the involvement of multiple chitosan molecules in the cross-linking of a single particle (12, 34).

In Equation 3, it was observed that the zeta potential increases with an increase in chitosan concentration. The ionic gelation method relies on the interaction between the protonated -NH3+ groups in the chitosan solution and the polyanionic phosphate groups in TPP. The zeta potential of chitosan nanoparticles is determined by the extent of unnaturalized -NH3+ groups in the presence of polyanionic phosphate groups. By increasing the chitosan concentration, there are more available -NH3+ groups in the chitosan solution. In comparison to nanoparticles with low chitosan concentration, nanoparticles with higher chitosan concentration may have more unnaturalized -NH3+ groups on their surfaces. Consequently, the zeta potential is expected to increase as the chitosan concentration increases (35).

The concentration of chitosan and TPP used in this study were capped at 0.20 %w/v and 0.08 %w/v, respectively. This is because aggregation will occur in chitosan nanoparticle formulations if the TPP used is more than the chitosan concentration (24) and this will lead to the formation of larger nanoparticles and a decrease in zeta potential (35). This can be observed by comparing Run #1 and Run #8, in which the increment of 0.02% of TPP has led to an increment in particle size (200.0 nm as compared to 465.4 nm) and a reduction of zeta potential (+37.8 mV as compared to +17.9 mV), despite using a lower concentration of chitosan, which theoretically should lead to smaller particle size.

From the result, the concentration of acetic acid should be at least 1.6 times higher than the concentration of chitosan to obtain a clear chitosan solution. This is consistent with the report from Fan et al. (2012) who described that the concentration of acetic acid used should be at least 1.5 times higher than chitosan concentration (12).

Drug molecules can be loaded in chitosan nanoparticles by two methods: incorporation method and incubation method. In the incorporation method, drug molecules will be premixed with chitosan solution and the

formation of drug-loaded chitosan nanoparticles will begin spontaneously when TPP is added to the drug-chitosan solution. This method will produce particles with entrapped/embedded drugs in the chitosan–drug nano-matrix, with some drug molecules being adsorbed on the surface of the nanoparticles. In the incubation method, chitosan nanoparticles will be formed first followed by incubation of the nanoparticles in the drug solution at predetermined concentrations. In this method, the drug will only be loaded via adsorption on the surface of the nanoparticles (36). The incorporation of active ingredients into nanoparticles could protect them from the harshness of the external environment. Additionally, the medications that have been trapped can be released under control, allowing a sustained release delivery for long-term therapy (37).

In general, the formulations with a 1:20 ratio produced the largest particle size when compared to another ratio in the same run number, whilst the formulas with a 1:100 ratio gave the smallest average particle size. This reflects the effect of ATQ concentration on the particle size; with the increment in drug concentrations, more of the drug molecules will be entrapped within and adsorbed on the surface of the chitosan nanoparticles, which leads to a dramatic increase in the particle size. The zeta potential on the other hand increases with a reduction in the drug concentration used, which could be due to a reduction in the amount of drug adsorbed on the nanoparticle's surface. The impact on PDI could also be observed, in which the uniformity of the particles reduces with the increment in drug concentration. This might be due to the adsorption of more drug molecules on the surface of the nanoparticles, thus affecting the uniformity index.

For all three runs, the highest EE (%) was demonstrated by a 1:100 ratio whilst the lowest was recorded by a 1:20 ratio. This indicates that the nanoparticles have an encapsulation limit, that could best be met with the 1:100 drug-to-CS ratio. Following the analysis conducted, Run #15 with a 1:100 ATQ: CS ratio was chosen to be further characterized in this study.

The FTIR spectra showed shifts of peaks in the spectrum of chitosan nanoparticles (blank) (c) comparing with the spectrum of chitosan flasks (b), in which the O-H/N-H vibration peak was shifted from 3427 cm–1 to 3448 cm–1. This shift was also previously reported in the literature (23, 38). The amide was also shifted to 1647 cm-1 from 1655 cm-1 and a new peak appeared at 1560 cm–1. This implies that complexes are formed through electrostatic interactions between chitosan NH3+ groups and TPP phosphoric groups within the nanoparticles, as described in previous studies (23, 39, 40).

The FTIR spectrum displayed all characteristic peaks of chitosan nanoparticles following the loading process of ATQ. However, the peaks corresponding to ATQ were not identifiable due to their overlap with the peaks of the nanoparticles. This overlap occurs because the concentration of nanoparticles is significantly higher than that of ATQ. Additionally, certain peaks exhibited a shift, such as the 1647 cm–1 peak being shifted to 1643 cm^{-1}, and the peak at 3448 cm–1 being shifted to 3439 cm^{-1}. These shifts can be attributed to the formation of new intermolecular hydrogen bonds between the chitosan nanoparticles and the drug molecules (41, 42).

The in vitro release behavior of ATQ-loaded nanoparticles (Run #15 with a 1:100 ratio of ATQ to CS) exhibited an initial burst release, as depicted in Figure 2 and Figure 3. Notably, the release of ATQ in SGF demonstrated a slower pace compared to SIF due to ATQ's higher solubility in basic media than in acidic media. The burst release phenomenon observed showed that approximately 50% of the loaded ATQ was released within the first 30 minutes. Subsequently, a more sustained release followed until six hours, when the release rate reached a plateau. This initial burst release from the chitosan nanoparticles can be attributed to two potential factors; the release of the adsorbed drug that is present on the surface of the nanoparticles, or due to the swelling of the polymers, which creates pores that enable the diffusion of the drug molecules from the polymer matrix. These factors collectively contribute to the release profile observed during the in vitro release study (43). Our results are consistent with the study of Alendronate sodium-loaded chitosan nanoparticles. Alendronate sodium is used to treat osteoporosis but has some limitations such as low oral bioavailability. In vitro drug release showed initial burst release followed by a prolonged release phase. more than half of the drug was released in 30 mins (44).

ATQ-loaded chitosan nanoparticles proved to be beneficial in improving the solubility of ATQ, with a remarkable 7-fold solubility enhancement in the SGF and 4-fold in the SIF, as compared to ATQ as a free drug. In SGF, ATQ-loaded nanoparticles achieved a remarkable drug release of 96.7% (±1.1%) within six hours, while in SIF, the nanoparticles demonstrated a release of 90.8% (±6.9%) within five hours. In contrast, the unformulated ATQ showed a limited solubility in both SGF and SIF, which was calculated as 29.3% (±4.1%) and 49.1% (±4.5%) respectively, in 24 hours. The results clearly indicate that the formulation of ATQ in chitosan nanoparticles enhances its solubility and facilitates a much higher and faster release of the drug in both SGF and SIF compared to the non-formulated ATQ. Chitosan nanoparticle formulation is hence a suitable approach to improve ATQ solubility and address the low solubility problem surrounding ATQ, which may potentially improve its bioavailability in vivo.

ATQ-loaded chitosan nanoparticles were dramatically affected at 40°C/75%RH storage condition during the stability study. The reduction in particle size at high temperatures was also reported by other studies (45) (46)

(12), which could be due to a decrease in chitosan's molar mass as a result of degradation that breaks the polymer chains and eventually causes a reduction in nanoparticles size and zeta potential. The reduction in drug content could be attributed to the interaction between the excipient and ATQ, which may cause the degradation of ATQ and lead to a reduction in the total drug content in the formulation under this condition.

CONCLUSION

Chitosan nanoparticles were successfully prepared by ionic gelation method and Design-Expert® software has assisted in understanding the effect of changing the concentration of the component (i.e., chitosan, acetic acid, and TPP) on the properties of chitosan nanoparticles produced. The final formulation of ATQ-loaded chitosan nanoparticles exhibits the following characteristics: a size of 235.9 nm (± 4.9), a PDI of 0.26 (± 0.02), a zeta potential of +29.2 mV (± 1.1), and an encapsulation efficiency of 95.0% (± 1.0). In vitro drug release study of ATQ-NP showed a 7-fold improvement in the solubility of ATQ in SGF, and a 4-fold in SIF when compared to the solubility of the free drug. Furthermore, the aqueous nanoparticle formulation demonstrates stability and can preserve the total drug content, with 98.5% (± 0.5%) and 94.4% (± 0.9%) of the drug concentration remains within the nanoparticles after three months of storage at 4°C and 25°C, respectively.

ACKNOWLEDGEMENT

The authors acknowledged the assistance of Ms. Kirtana Supramaniam, Mr. Mohd Asro Ramli and Mr. Jusfaridan Aizan in this work.

REFERENCES

1. Calvo J, Lavandera JL, Agüeros M, Irache JM. Cyclodextrin/poly (anhydride) nanoparticles as drug carriers for the oral delivery of atovaquone. Biomedical microdevices. 2011;13(6):1015-25
2. Fiorillo M, Lamb R, Tanowitz HB, Mutti L, Krstic-Demonacos M, Cappello AR. Repurposing atovaquone: targeting mitochondrial complex III and OXPHOS to eradicate cancer stem cells. Oncotarget. 2016;7(23):34084
3. McKeage K, Scott LJ. Atovaquone/proguanil. Drugs. 2003;63(6):597-623
4. Basselin M, Hunt SM, Abdala-Valencia H, Kaneshiro ES. Ubiquinone synthesis in mitochondrial and microsomal subcellular fractions of Pneumocystis spp.: differential sensitivities to atovaquone. Eukaryotic Cell. 2005;4(8):1483-92
5. Fry M, Pudney M. Site of action of the antimalarial hydroxynaphthoquinone, 2-[trans-4-(4'-chlorophenyl) cyclohexyl]-3-hydroxy-1, 4-naphthoquinone (566C80). Biochemical pharmacology. 1992;43(7):1545-53
6. Srivastava IK, Rottenberg H, Vaidya AB. Atovaquone, a broad spectrum antiparasitic drug, collapses mitochondrial membrane potential in a malarial parasite. Journal of Biological Chemistry. 1997;272(7):3961-6
7. Kathpalia H, Juvekar S, Shidhaye S. Design and in vitro evaluation of atovaquone nanosuspension prepared by pH based and anti-solvent based precipitation method. Colloid and Interface Science Communications. 2019;29:26-32
8. Borhade V, Pathak S, Sharma S, Patravale V. Formulation and characterization of atovaquone nanosuspension for improved oral delivery in the treatment of malaria. Nanomedicine. 2014;9(5):649-66
9. Malpezzi L, Fuganti C, Maccaroni E, Masciocchi N, Nardi A. Thermal and structural characterization of two polymorphs of Atovaquone and of its chloro derivative. Journal of thermal analysis and calorimetry. 2010;102(1):203-10
10. Chae SY, Jang M-K, Nah J-W. Influence of molecular weight on oral absorption of water soluble chitosans. Journal of Controlled Release. 2005;102(2):383-94
11. Kumar MNR. A review of chitin and chitosan applications. Reactive And Functional Polymers. 2000;46(1):1-27
12. Fan W, Yan W, Xu Z, Ni H. Formation mechanism of monodisperse, low molecular weight chitosan nanoparticles by ionic gelation technique. Colloids and Surfaces B: Biointerfaces. 2012;90:21-7
13. Pan C, Qian J, Fan J, Guo H, Gou L, Yang H, et al. Preparation nanoparticle by ionic cross-linked emulsified chitosan and its antibacterial activity. Colloids and Surfaces A: Physicochemical and Engineering Aspects. 2019;568:362-70
14. Gomathi T, Sudha P, Florence JAK, Venkatesan J, Anil S. Fabrication of letrozole formulation using chitosan nanoparticles through ionic gelation method. International journal of biological macromolecules. 2017;104:1820-32
15. Ciro Y, Rojas J, Alhajj MJ, Carabali GA, Salamanca CH. Production and characterization of chitosan–polyanion nanoparticles by polyelectrolyte complexation assisted by high-intensity sonication for the modified release of methotrexate. Pharmaceuticals. 2020;13(1):11
16. Jiang L, Duan H, Ji X, Wang T, Wang Y, Qiu J. Application of a simple desolvation method to increase the formation yield, physical stability and hydrophobic drug encapsulation capacity of chitosan-based nanoparticles. International journal of pharmaceutics. 2018;545(1-2):117-27
17. Kafshgari MH, Khorram M, Mansouri M, Samimi A, Osfouri S. Preparation of alginate and chitosan nanoparticles using a new reverse micellar system. Iranian Polymer Journal. 2012;21(2):99-107
18. Debnath S, Kumar RS, Babu MN. Ionotropic gelation–a novel method to prepare chitosan

nanoparticles. Research Journal of Pharmacy and Technology. 2011;4:492-5
19. Calvo P, Remunan-Lopez C, Vila-Jato JL, Alonso M. Novel hydrophilic chitosan-polyethylene oxide nanoparticles as protein carriers. Journal of Applied Polymer Science. 1997;63(1):125-32
20. Grenha A. Chitosan nanoparticles: a survey of preparation methods. Journal of Drug Targeting. 2012;20(4):291-300
21. de Pinho Neves AL, Milioli CC, Müller L, Riella HG, Kuhnen NC, Stulzer HK. Factorial design as tool in chitosan nanoparticles development by ionic gelation technique. Colloids and Surfaces A: Physicochemical and Engineering Aspects. 2014;445:34-9
22. Sullivan DJ, Cruz-Romero M, Collins T, Cummins E, Kerry JP, Morris MA. Synthesis of monodisperse chitosan nanoparticles. Food Hydrocolloids. 2018;83:355-64
23. Ruslan NS, Mohtar N, Rahiman SSF, Gazzali AM. The Influence of Preparation Factors on Physical Characteristics of Chitosan Nanoparticles. Journal of Physical Science. 2020;31(3):47-60
24. Agarwal M, Agarwal MK, Shrivastav N, Pandey S, Das R, Gaur P. Preparation of chitosan nanoparticles and their in-vitro characterization. International Journal of Life-Sciences Scientific Research. 2018;4(2):1713-20
25. Mohtar N, Khan NA, Darwis Y. Solid lipid nanoparticles of atovaquone based on 24 full-factorial design. Iranian journal of pharmaceutical research: IJPR. 2015;14(4):989
26. Meng Y, Yao C, Xue S, Yang H. Application of Fourier transform infrared (FT-IR) spectroscopy in determination of microalgal compositions. Bioresource Technology. 2014;151:347-54 https://doi.org/10.1016/j.biortech.2013.10.064.
27. Knipe JM, Strong LE, Peppas NA. Enzyme-and pH-responsive microencapsulated nanogels for oral delivery of siRNA to induce TNF-α knockdown in the intestine. Biomacromolecules. 2016;17(3):788-97
28. Stuart AV, Clement Y, Sealy P, Löbenberg R, Montane-Jaime L, Maharaj R, et al. Comparing the dissolution profiles of seven metformin formulations in simulated intestinal fluid. Dissolution Technologies. 2015;22(1):17-22
29. Bahiraei M, Derakhshandeh K, Mahjub R. Hydrophobic ion pairing with cationic derivatives of α-, ß-, and γ-cyclodextrin as a novel approach for development of a self-nano-emulsifying drug delivery system (SNEDDS) for oral delivery of heparin. Drug Development and Industrial Pharmacy. 2022:1-15
30. Bolmal UB, Hj P. Formulation of atovaquone tablet using biosurfactant in a ternary solid dispersion system: In vitro and in vivo evaluation. International Journal of Applied Pharmaceutics. 2019;11(2):44-9
31. Darade A, Pathak S, Sharma S, Patravale V. Atovaquone oral bioavailability enhancement using electrospraying technology. European Journal of Pharmaceutical Sciences. 2018;111:195-204
32. Bezerra MA, Lemos VA, Novaes CG, de Jesus RM, Souza Filho HR, Araújo SA, et al. Application of mixture design in analytical chemistry. Microchemical Journal. 2020;152:104336
33. Buruk Sahin Y, Aktar Demirtaş E, Burnak N. Mixture design: A review of recent applications in the food industry. Pamukkale University Journal of Engineering Sciences. 2016
34. Hussain Z, Sahudin S. Preparation, characterisation and colloidal stability of chitosan-tripolyphosphate nanoparticles: optimisation of formulation and process parameters. International Journal of Pharmacy and Pharmaceutical Sciences. 2016;8(3):297-308
35. Hu B, Pan C, Sun Y, Hou Z, Ye H, Hu B, et al. Optimization of fabrication parameters to produce chitosan– tripolyphosphate nanoparticles for delivery of tea catechins. Journal Of Agricultural And Food Chemistry. 2008;56(16):7451-8
36. Gan Q, Wang T. Chitosan nanoparticle as protein delivery carrier—systematic examination of fabrication conditions for efficient loading and release. Colloids and Surfaces B: Biointerfaces. 2007;59(1):24-34
37. Bugnicourt L, Ladavière C. Interests of chitosan nanoparticles ionically cross-linked with tripolyphosphate for biomedical applications. Progress in polymer science. 2016;60:1-17
38. Papadimitriou S, Bikiaris D, Avgoustakis K, Karavas E, Georgarakis M. Chitosan nanoparticles loaded with dorzolamide and pramipexole. Carbohydrate polymers. 2008;73(1):44-54
39. Hosseini SF, Zandi M, Rezaei M, Farahmandghavi F. Two-step method for encapsulation of oregano essential oil in chitosan nanoparticles: Preparation, characterization and in vitro release study. Carbohydrate Polymers. 2013;95(1):50-6
40. Gomathi T, Sudha PN, Florence JAK, Venkatesan J, Anil S. Fabrication of letrozole formulation using chitosan nanoparticles through ionic gelation method. International Journal of Biological Macromolecules. 2017;104:1820-32
41. Joseph JJ, Sangeetha D, Gomathi T. Sunitinib loaded chitosan nanoparticles formulation and its evaluation. International journal of biological macromolecules. 2016;82:952-8
42. Lazaridou M, Christodoulou E, Nerantzaki M, Kostoglou M, Lambropoulou DA, Katsarou A. Formulation and in-vitro characterization of chitosan-nanoparticles loaded with the iron chelator deferoxamine mesylate (DFO). Pharmaceutics. 2020;12(3):238
43. Mohammed MA, Syeda JT, Wasan KM, Wasan EK. An overview of chitosan nanoparticles and its application in non-parenteral drug delivery.

Pharmaceutics. 2017;9(4):53
44. Miladi K, Sfar S, Fessi H, Elaissari A. Enhancement of alendronate encapsulation in chitosan nanoparticles. Journal of Drug Delivery Science and Technology. 2015;30:391-6
45. Morris GA, Castile J, Smith A, Adams GG, Harding SE. The effect of prolonged storage at different temperatures on the particle size distribution of tripolyphosphate (TPP)–chitosan nanoparticles. Carbohydrate polymers. 2011;84(4):1430-4
46. Jang K-I, Lee HG. Stability of chitosan nanoparticles for L-ascorbic acid during heat treatment in aqueous solution. Journal of agricultural and food chemistry. 2008;56(6):1936-41